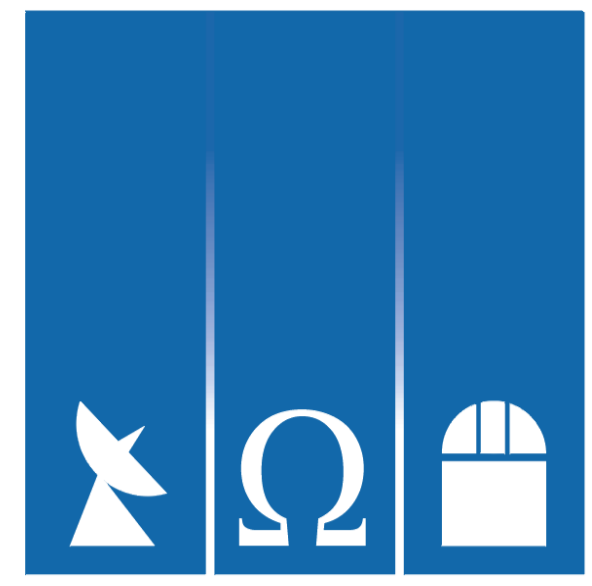


Strong gravitational lensing in RX J1347-1145



Argelander-
Institut
für
Astronomie

Alexi Halkola¹, Thomas Erben¹, Hendrik Hildebrandt¹, Marco Lombardi²,
Tim Schrabback-Krahe¹

¹Argelander-Institut für Astronomie, Auf dem Hügel 71, 53121 Bonn, Germany

²European Southern Observatory, Karl-Schwarzschild-Straße 2, 85748 Garching, Germany

Abstract

As the most X-ray luminous cluster identified on the sky (Schindler et al. 95), RXJ1347 is also a promising cluster for a detailed strong lensing analysis. In ground based images several tentative arcs and multiple images have been observed (e.g. Schindler et al. 95, Sahu et al. 98, Bradac et al. 05). The cluster has been studied in X-rays (e.g. Schindler et al. 97, Allen et al. 02, Gitti et al. 07), SZ effect (e.g. Pointecouteau et al. 01), spectroscopically (Sahu et al. 98, Cohen et al. 02), with weak lensing (Fischer et al. 97, Kling et al. 05). Strong lensing analyses include Sahu et al. 98 and Bradac et al. 05. The analysis of Bradac et al. combined both strong and weak lensing to constrain the mass profile of the cluster. Recent ACS observations of the cluster in 3 bands have enabled us to identify several new image systems, crucially also a 5 image system. Follow up spectroscopic observations at the VLT FORS2 have confirmed that the long debated giant arc forms a multiple images system with the southern blue arc. A mass modelling based on the two image arc system with a redshift of 1.75 and the 5 image system allows us to determine the mass profile of the cluster with high accuracy. The projected mass profile is well fit by either a non-singular isothermal sphere with $\sigma = 1935 \pm 40$ km/s and $r_c = 20 \pm 2''$, or a Navarro, Frenk and White profile with $C = 5.4 \pm 0.7$ and $r_{200} = 3.3 \pm 0.2$ Mpc.

Data

We have used both ground and spacebased imaging in order to search for multiple images and constrain their properties. FORS and WFI images in UBVRI bands are used to obtain photometric redshifts for the galaxies (Bradac et al. 05). The photometric redshift probability densities are also used to check that all multiple image systems are consistent. The high spatial resolution and limited colour information of the ACS images (F475W, F814W, F850LP) is used to find the multiple images and check that the colours match although the bands are not enough to obtain secure redshifts. We have also obtained spectra on FORS2 for the multiple image candidates as well as many other galaxies both in the cluster and in the background in order to identify cluster galaxies and calibrate photometric redshifts.

Multiple image systems

We have identified 13 galaxies that are probably strongly lensed. These are marked on fig. 1. Although most of these are two image systems near critical lines we have also found a 5 image system that is crucial for the mass modelling. With the FORS2 spectra we have been able to confirm a redshift of 1.75 for the two images in image system 2, an arc system that has been identified already in ground based images and now finally confirmed.

Mass components

The strong lensing mass models are made up of the small scale structure in the galaxies and a smoothly distributed component with dark matter and hot X-ray gas. The galaxies are modelled with truncated isothermal spheres. Their velocity dispersions are estimated from their luminosity via the Faber-Jackson relation. The truncation radii of galaxies are poorly constrained and we therefore assume the same scaling law between the truncation radius s of a galaxy and its velocity dispersion σ as was found for A1689 in Halkola et al. 2007 ($s = 56 \text{ kpc} \times \sigma / 220 \text{ km/s}$).

The smooth component is described by 2 haloes that have either NSIE or ENFW profile.

Markov chain Monte Carlo

We estimate the 2-dimensional mass map and its error using a Markov chain Monte Carlo method. The random sampling of the MCMC method allows us to effectively sample the parameter space and to robustly estimate the error on the mass map, not only the regions of low chi-squared. With the MCMC analysis we also take into account the uncertainty in the galaxy component of the cluster.

References:

Allen et al., 2002, MNRAS 335, 256
Bradac et al. 2005, A&A 437, 49
Cohen et al. 2002, ApJ 573, 524
Fischer et al. 1997, AJ 114, 14

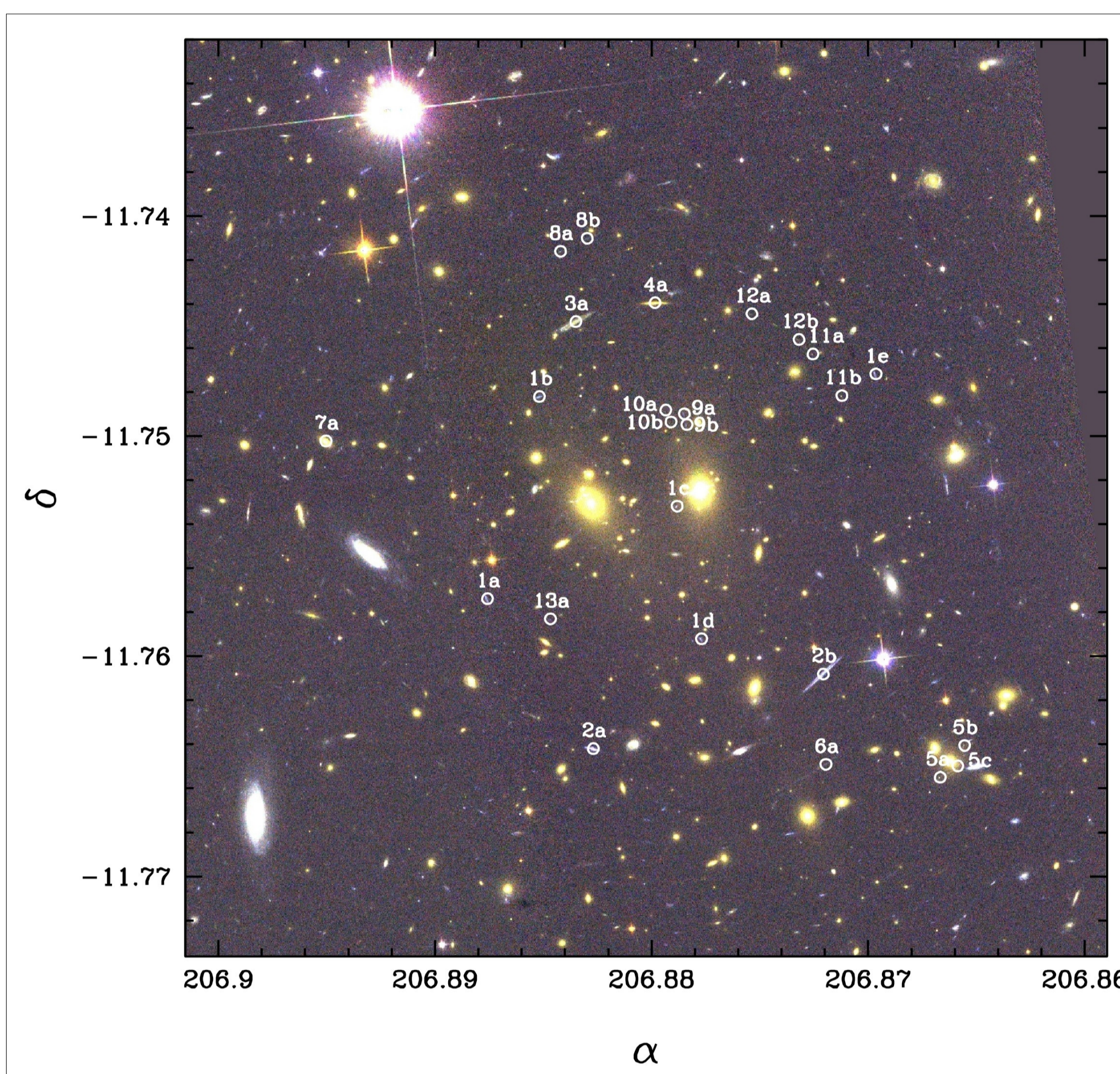


Fig. 1.— Multiple image systems in RX J1347-1145. 13 multiple image systems are identified. However only image systems 1 and 2 are used to constrain the mass profile. Image system 1 is a 5 image system with a broad photometric redshift probability distribution between 0.5 and 2.0. Image system 2 has a spectroscopic redshift of 1.75. The other image systems have mainly 2 images and are well reproduced by finding an appropriate redshift for the systems.

Kappa map

The average kappa map of the cluster is shown in Fig. 2. The peak of the mass distribution is between the two bright central galaxies. The kappa map is also clearly elliptical with elongation along the NNE direction.

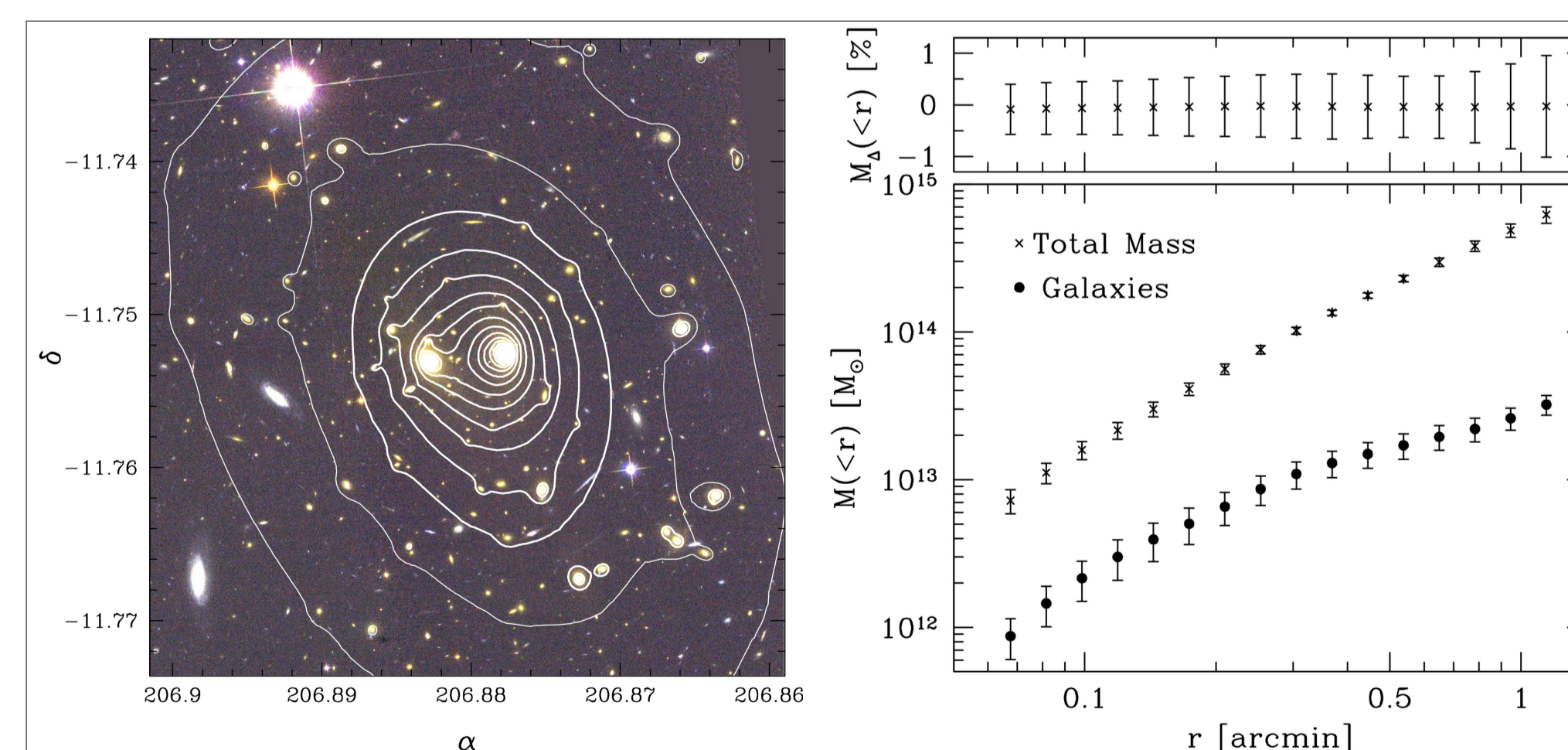


Fig. 2.— On the right panel we show the average kappa map of the cluster. The thick contours show the kappa = 1.00, 1.25, 1.50... contours, while the thin contours show the kappa = 0.75, 0.50, 0.25 levels. On the left hand side the radial mass profile can be seen. The crosses show the total mass, circles the mass in the galaxies. The top panel on the right shows the 'residual' mass of the cluster as a percentage of the total mass.

Radial mass profile

The radial mass profile of the cluster is given in Fig. 2. The total mass is shown as crosses on the bottom part of the right panel. In addition to the total mass we also plot the contribution from the galaxies with circles. Galaxies have typically $\sim 10\%$ of the total mass of the cluster. The top part of the panel shows the residual mass (for more details see the Residual mass box below). All errors shown are the 1-sigma errors from the MCMC analysis.

The total mass is well fitted by both an NSIS and NFW profile. The 1-, 2- and 3-sigma confidence contours are shown in Fig. 3, the best fit values are marked by crosses. The best fit parameters are $\sigma = 1935 \pm 40$ km/s and $r_c = 20 \pm 2''$ for the NSIS profile, or $C = 5.4 \pm 0.7$ and $r_{200} = 3.2 \pm 0.2$ Mpc for the NFW profile. The cluster is obviously very massive but one should keep in mind that the core radius of the NSIS lessens the mass when compared to a singular isothermal sphere with the same velocity dispersion. Similarly the large r_{200} of the NFW halo does not reflect the true r_{200} of the cluster as that requires extrapolation beyond the strong lensing region.

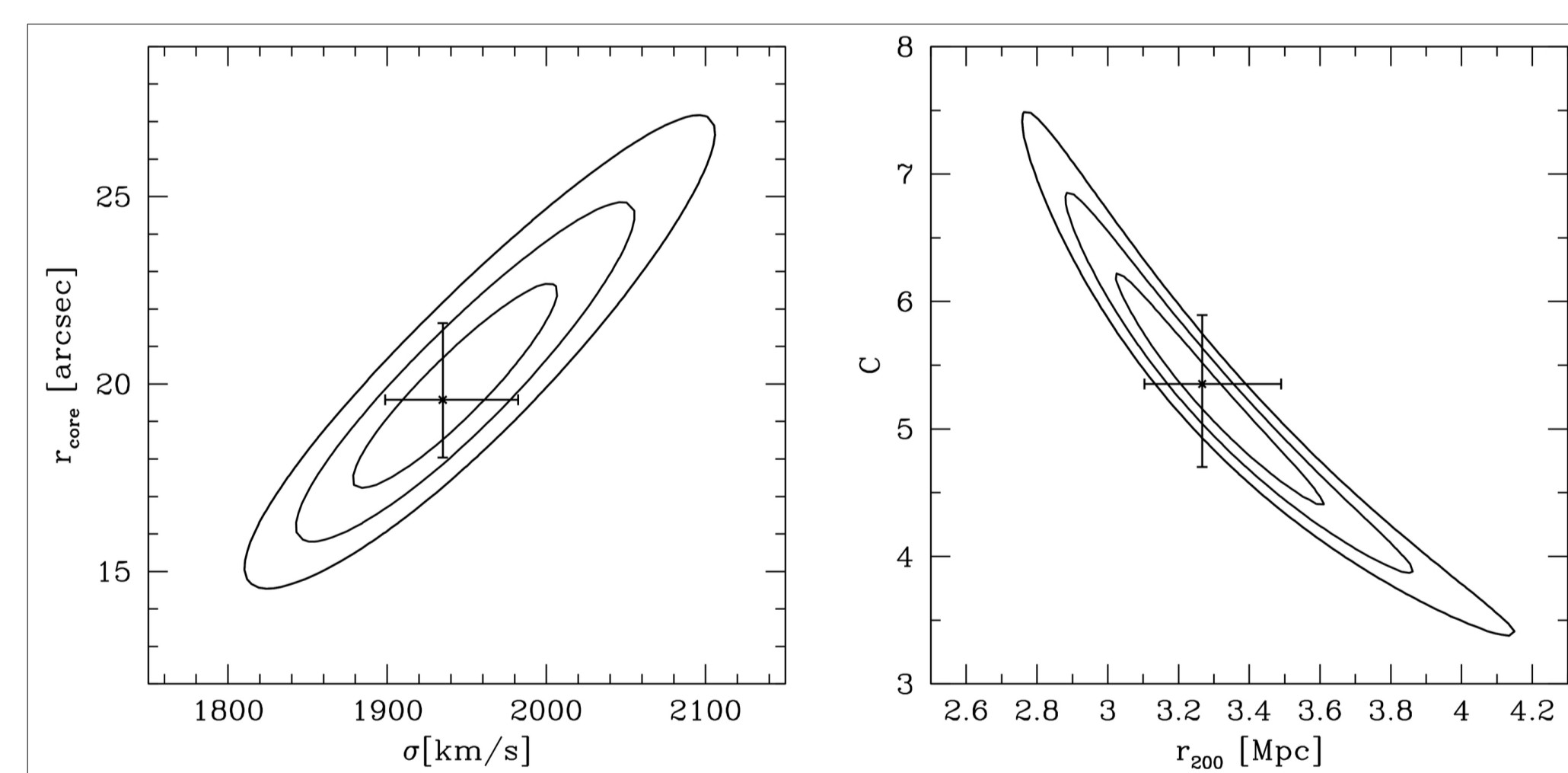


Fig. 3.— The 1-, 2-, and 3-sigma confidence contours for the NSIE and NFW halo fits to the total mass. The best fit values and marginalised error bars are also given. These are $\sigma = 1935 \pm 40$ km/s and $r_c = 20 \pm 2''$ for the NSIE profile, or $C = 5.4 \pm 0.7$ and $r_{200} = 3.3 \pm 0.2$ Mpc for the NFW profile.

Residual mass

In the presence of measurement errors and model assumptions it is natural that the images are not reproduced exactly. Inspired by LensPerfect by Dan Coe we have calculated a residual mass map necessary to perfectly fit the data. The radial profile of 'residual' mass of the cluster is shown on the top of the right panel in Fig. 2. It is consistent with 0% at all radii of the cluster and has a scatter of at most 1%. This shows that our lensing modelling is not biased to lower or higher masses as the images can be reproduced with out net change in the total mass.

Pointecouteau et al. 2001, ApJ 552, 42
Sahu et al. 1998, ApJ, 492, L125
Schindler et al. 1995, A&A 299, L9
Schindler et al. 1997, AAP 317, 649

Gitti et al. 2007, Astro-ph 0706.3001v1
Halkola et al. 2006, MNRAS 372, 1425
Halkola et al. 2007, ApJ 656, 739
Kling et al. 2005, ApJ 625, 643